Contactless Acoustic Manipulation and Sorting of Particles by Dynamic Acoustic Fields

Marco A. B. Andrade, George D. Skotis, Scott Ritchie, David R. S. Cumming, Mathis O. Riehle, and Anne L. Bernassau

***Abstract*—This paper presents a contactless, acoustic technique to manipulate and sort particles of varying size in both liquid and air media. An acoustic standing wave is generated by the superposition of counter-propagating waves emitted by two opposing emitters. The acoustic radiation force traps the smallest particles at the pressure nodes of the acoustic standing wave. The position of the particles can be manipulated by dynamically changing the phase difference between the two emitters. By applying a dynamic acoustic field (DAF), it is demonstrated that particles can be manipulated spatially and sorted according to size. The discrimination (sorting dynamic range) capability is initially demonstrated in liquid media by separating three different sets of polystyrene particles, ranging in size from 5 to 45 μm in diameter. The separation between particles was performed up to a ratio of 5/6 in diameter (20 % diameter difference). Finally, the scalability of the DAF method is demonstrated by sorting expanded polystyrene particles of 2 and 5 mm diameter in air.**

I. Introduction

TRAPPING, manipulation, and sorting of particles by contactless methods have a wide range of applications in biology, medicine, chemistry and in the industry. Applications include the manipulation [1] and sorting of cells [2], [3], contactless handling of chemical substances [4], sorting of bio-aerosol particles [5], etc. Nowadays, numerous methods are available to manipulate and sort particles, such as magnetic [6], dielectric [7], optical [8], and acoustic [9]. Among these methods, acoustic manipulation techniques have the advantage of working with any material [9] no matter their electric or magnetic properties. The contactless nature of acoustic manipulation allows operation in a complete non-contaminating fashion, or conversely, to operate on highly contaminating substances or living organisms. In our previous work, temperature and cell viability of the acoustic tweezers were assessed [10], [11]. Finally, acoustic manipulation and separation of particles has been classically performed using a static acoustic field [12], [13]. Recently dynamic [1], [14] acoustic fields have shown enhanced capabilities as well as opened new possibilities in acoustic manipulations. These dynamic field technologies can be implemented by several methods. It has been previously demonstrated that one emitter and a reflector can be used to create a standing wave that traps particles in fixed positions in space [15]-[17]. With this technology, it is possible to trap particles and transport them by changing the driving frequency [18], [19]. However, this method presents several challenges, such as an unstable force resulting in movement among trapped particles. A different strategy to manipulate particles uses two acoustic emitters producing counter-propagating waves as demonstrated in liquid by Grinenko *et al.* [20]. The superposition between these two propagating waves, results in a standing acoustic wave with fixed pressure nodes where the particles can be trapped. The pressure nodes and thus the trapping positions can be translated and adjusted by changing the phase difference between the two emitters [21]. This technique has been applied in air [21] and in liquid media [20], [22]. In the ideal case, the wave generated by one sound emitter should be completely absorbed by the opposite emitter. If this is not the case, unwanted waves e.g. reflected by the emitter surface can superimpose on the acoustic standing wave, reducing the manipulation capability and interfering with the trapping process. In practice, acoustic manipulation can only be achieved when the reflection coefficient of the emitters is lower than 0.5 [20]. In the case of particle manipulation in liquid media, the reflection coefficient can be minimized by using piezoelectric transducers with matching and absorbing backing layers [20], [23]. However, the large mismatch between the acoustic impedance of air and the transducer materials makes the minimization of the reflection coefficient difficult to achieve. To address this problem, Kozuka and co-authors [21] used two angled transducers to reduce the wave reflection by the opposite transducer, but this strategy has the disadvantage of only allowing manipulation over short distances.

In this paper, we demonstrate a scalable and tunable technique that can be used to not only manipulate but also simultaneously separate particles by size. This technology uses dynamic acoustic fields (DAFs). This technology can adapt to the particles that need to be discriminated but also can be scaled to larger systems. We demonstrate the tunability of the system and the discrimination power of our method by

Part of this work was supported by an EPSRC EFutures grant (RES/0560/7386) and a Royal Society Research grant (RG130493). Support from GU68 Engineers Trust of the United Kingdom and São Paulo Research Foundation - FAPESP (grant #2014/24159-1) are gratefully acknowledged.

M.A.B. Andrade is with the Institute of Physics, University of São Paulo, Brazil

G.D. Skotis, S. Ritchie, and D.R.S. Cumming is with School of Engineering, University of Glasgow, UK.

M.O Riehle is with the Institute of Molecular, Cell and Systems Biology, University of Glasgow, UK.

A.L. Bernassau is with the School of Engineering and Physical Sciences, Heriot-Watt University, UK (e-mail: a.bernassau@hw.ac.uk).

testing it on a mixture of polystyrene particles of lower and lower diameter difference (45-10, 10-8 and 6-5 μm) in liquid media. Finally, to demonstrate the generality of the DAF technique, we demonstrate the manipulation and separation of polystyrene particles of 2 and 5 mm diameter in air.

II. DYNAMIC ACOUSTIC FIELD TECHNIQUE

The DAF technique relies in generating a time-controlled standing wave through the superposition of counter-propagating waves produced by two opposite emitters, where the phase difference between emitters is time-varied by computer control. Assuming a planar standing wave, the primary acoustic radiation force F_a, which acts on a small spherical particle of radius R, can be expressed by [12], [24]:

$$F_a = -\left(\frac{2\pi^2 p_0^2 R^3 \beta_w}{3\lambda}\right)\phi(\beta,\rho)\sin(2kx+\theta)\,, \tag{1}$$

where p_0 is the acoustic pressure amplitude, θ is the phase difference between the emitters, λ is the wavelength, $k = 2\pi/\lambda$ is the wave number, x is the distance from a pressure node, and $\phi(\beta,\rho)$ is the acoustic contrast factor, given by:

$$\phi(\beta,\rho) = \frac{5\rho_c - 2\rho_w}{2\rho_c + \rho_w} - \frac{\beta_c}{\beta_w}\,. \tag{2}$$

The acoustic contrast factor $\phi(\beta,\rho)$ depends on the mechanical properties of the particle and the surrounding fluid, where ρ is the density, β is the compressibility, and the subscripts c and w refer to the properties of the particle and of the fluid, respectively. The sign of the acoustic contrast factor determines the direction of the acoustic radiation force. If the contrast factor is positive, the acoustic radiation force causes the particles to move to the pressure nodes, while a negative contrast factor causes the particles to move to the pressure antinodes. In the particular case of a standing wave in air, the contrast factor is positive, which has the consequence of attracting particles to the pressure nodes.

A spherical particle moving through a fluid, also experiences a viscous drag force F_v. For small relative velocities (Stokes flow) between the particles and the fluid, the viscous drag force is given by:

$$F_v = -6\pi\eta R u\,, \tag{3}$$

where η is the medium viscosity, R is the particle radius, and u is the relative velocity between the particle and the fluid.

When θ is altered, the positions of the pressure nodes are translated along the x-axis. In a quasi-static condition, the viscous drag force is much smaller than the acoustic radiation force, and particles of positive contrast factor follow the position of a moving node. However, if the phase difference between the emitters is changed rapidly, the viscous drag force becomes significant, causing some particles to follow a moving node and other particles to remain close to their initial position. The tendency of a particle to follow a moving node or not depends on the interplay of the acoustic and the drag forces, i.e. on the rate at which the phase difference is altered, the size of the particle, and on the mechanical properties of the particle and of the host media. This allows particles to be separated as a function of size, density, and compressibility. The use of the DAF technique to separate particles by size is illustrated in Fig. 1. The technique relies on a repeated cycling pattern of the phase difference between two excited transducers from 0 to 360° (Fig. 1(a)). Within each cycle, the phase is swept completely through 360° over time t_{ramp} and then allowed to rest for time t_{rest}. This pattern is repeated over and over. The core of the DAF technique is based on the relationship between the rate at which the phase is swept, t_{ramp}, during which time the particles are moved, and the length of t_{rest} during which time larger particles stabilize in their new position and smaller particles relax back into their initial position. If at the end of the t_{ramp} period, the smaller particles have not travelled more than halfway (antinode) from their initial node position to the next node position, they will relax back to their starting position during t_{rest}, whereas the particles of interest, which have travelled past the antinode between the initial node and the next node, will relax towards the next node position.

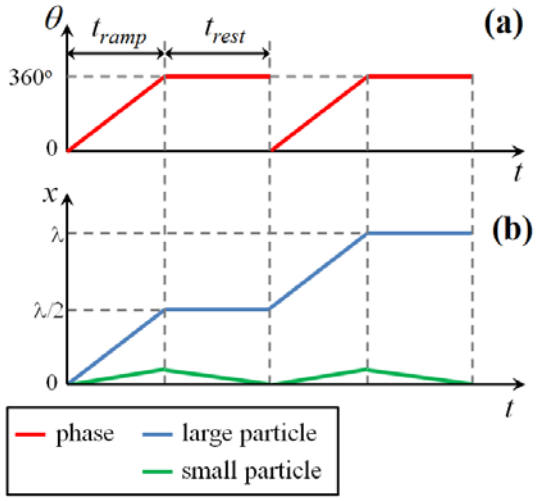

Fig. 1. A schematic diagram of (a) the phase shift pattern t_{ramp}, t_{rest} (see text). (b) The corresponding effect on large and small particles. The larger particles follow the node, thus when the phase shift reaches the rest period at 360°, the large particles have reached the position of the next acoustic pressure node. In contrast, however, the smaller particles have only been displaced by a small amount and can relax back to their initial position during t_{rest}.

A. DAF Simulation

To obtain a better understanding of how different parameters affect the separation of particles, a finite-difference scheme is applied to simulate the particle motion under a dynamic acoustic field. In this scheme, the horizontal position $x(t)$ and the velocity $u(t)$ of a particle are determined by:

$$x(t+\Delta t) = x(t) + u(t)\Delta t + \frac{1}{2}a(t)\Delta t^2\,, \tag{4}$$

$$u(t+\Delta t) = u(t) + a(t)\Delta t\,, \tag{5}$$

where Δt is the time step and the particle acceleration $a(t)$ is calculated by:

$$a(t) = \frac{F_a + F_v}{m}\,. \tag{6}$$

In (6), m is the particle mass and the acoustic radiation force F_a is given by (1). In the experiments in water, the highest Reynolds number Re is on the order of 1 x 10^{-3} and the viscous drag force F_v is calculated by using (3).

The determination of the acoustic radiation force F_a, given by (1) is valid for plane standing waves. When a small particle is located in an arbitrary acoustic field, a more general equation is required to obtain the acoustic radiation force.

According to Gor'kov [25], the acoustic radiation force that acts on a sphere with a radius R, which is much smaller than the wavelength, is calculated by:

$$\mathbf{F} = -\nabla U\,, \tag{7}$$

where the Gor'kov potential U is given by [25]:

$$U = 2\pi R^3 \left[\frac{\langle p^2 \rangle}{3\rho c^2} - \frac{\rho \langle u^2 \rangle}{2} \right], \tag{8}$$

In (8), ρ is the air density, c is the sound velocity in air and the symbol $\langle\ \rangle$ denotes the time average over a period. It is also assumed that the particle is rigid, which is a good assumption for particles immersed in an air medium. The dimensionless form of U is considered, which is calculated by [15]

$$\tilde{U} = \frac{U}{2\pi R^3 \rho u_0^2}\,, \tag{9}$$

where u_0 is the velocity amplitude of the vibrating source. In the presence of an acoustic standing wave, small particles are attracted to the pressures nodes, which coincide with the positions of the minimum Gor'kov potential. In this paper, the Gor'kov equation, given by (8), was applied with the main purpose of determining the positions of minimum potential, and not the acoustic radiation force that acts on the particles.

III. EXPERIMENTAL SETUP

A. Device for particle manipulation in liquids

Manipulation and sorting of particles of various sizes in liquid media are performed by using the experimental setup illustrated in Fig. 2. This setup is formed by an octagonal cell with 8 piezoelectric transducers located at opposing sides [22]. This cell was previously characterized and allows contactless manipulation in two dimensions. In the present paper, only two opposing transducers are used in the experiments, and consequently, the particle manipulation is restricted to the one-dimensional case. Although the experiments were performed with an octagonal cell, any other shape capable of producing two counter-propagating waves could be applied. As described previously [22], the transducers matching layer was optimized to minimize the reflection of the incident wave emitted by the opposite transducer. In the experiments, the two transducers were excited by a multi-channel function generator (TGA12104, Aim and Thurlby Thandar Instruments, UK) and the generated signals were amplified and electronically matched by high speed buffers (BUF634T, Texas Instruments, USA). A control interface developed in LabVIEW (National Instruments, UK) allows controlling the phase difference between transducers, and consequently, the manipulation of the particles horizontally. An agar layer was introduced at the bottom of the octagonal cavity, allowing the minimization of the acoustic streaming [26], and consequently reducing its influence on the movement of small particles without disturbing the acoustic field inside the cavity.

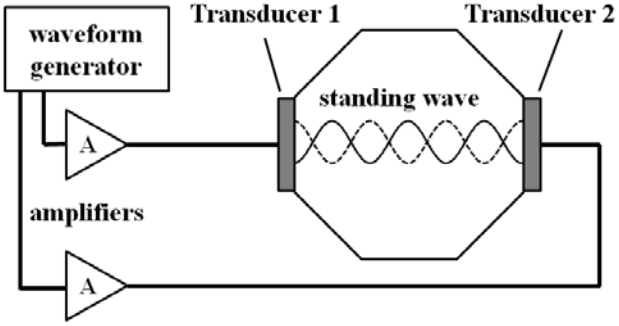

Fig. 2. A schematic diagram of the experimental setup for the manipulation and sorting of particles in liquid media.

B. Device for particle manipulation in air

To demonstrate how DAF could be applied to the contactless manipulation and sorting of particles in air, an acoustic system was built with two compression driven loudspeakers (BMS 4550 model, Germany). A glass plate was introduced between the two loudspeakers to support the particles. Synchronisation between channels was achieved using an arbitrary waveform generator (TGA12104, Aim and Thurlby Thandar Instruments, UK) allowing independent control of the amplitude, phase, and frequency of each channel. The signals from the waveform generators were amplified by an audio amplifier (LA50b, Prism Audio, UK). The system was controlled by a virtual control panel developed in LabVIEW (National Instruments, UK), which automatically varied all parameters in real time and hence produce the DAF. The arbitrary waveform generator uses the direct digital synthesis (DDS) technology resulting in an uneven change of amplitude when the phase of the exciting signal is modulated (supplementary video 1). The voltage spikes apparent on the generator model causes destabilization of the particles in the dynamic acoustic field. The LabVIEW interface was designed to facilitate manipulation and was essential to achieve sorting of the particles in air. A schematic diagram of the air manipulation device is presented in Fig. 3.

The acoustic device was simulated by employing a numerical model that combined a three-dimensional finite element method (FEM) with the Gor'kov equation [25]. To simplify the FEM model, the loudspeakers were modeled as circular planar pistons with a diameter of 25 mm that vibrate uniformly with the velocity amplitude u_0 at a frequency of 17.5 kHz. The FEM simulations were carried out in the commercial software ANSYS (ANSYS Inc., Canonsburg, PA), where acoustic fluid elements were used to model the wave propagation in air, and structural elements were used to model the transducer, walls, and the horizontal glass plate. The coupling between the acoustic fluid and structural elements is performed by using elements with fluid-structure interaction capability. First, the FEM determined the acoustic pressure p and velocity-distribution u in space. Then, these two fields were exported to Matlab (MathWorks, Natick, MA), where they were introduced into the Gor'kov equation to obtain the potential of the acoustic radiation force that acts on a small sphere.

In order to address the problem of wave reflections by the opposite speakers, FEM simulations were carried out and it was verified that, depending on the distance between the vertical walls that surround the speakers, it is possible to reduce the wave reflection and thus prevent the formation of a standing wave when only one speaker is turned on. To perform this analysis, the FEM was applied to determine the acoustic pressure distribution between the parallel walls as a function of the distance L between walls. In this analysis, only the left speaker emits a sound wave. The result of this analysis is presented in Fig. 4, which shows the numerical dimensionless acoustic pressure distribution (calculated by $\tilde{p} = p/\rho c v_0$) as a function of x and L. The acoustic pressure was determined along a horizontal line located 2 mm above the glass plate, with the origin of the x-axis coinciding with the surface of the left wall.

The results in Fig. 4 show that, depending on L, an acoustic standing wave is formed even though the speaker on the right is turned off. To avoid this, the distance between the walls should be adjusted to a specific value. In our device, a distance of 62 mm between the walls was chosen, represented by the horizontal dashed line in Fig. 4. It was verified numerically that, for L = 62 mm, the acoustic standing wave was produced only when both speakers were excited simultaneously. In this case, particles could be manipulated by changing the phase difference between the speakers.

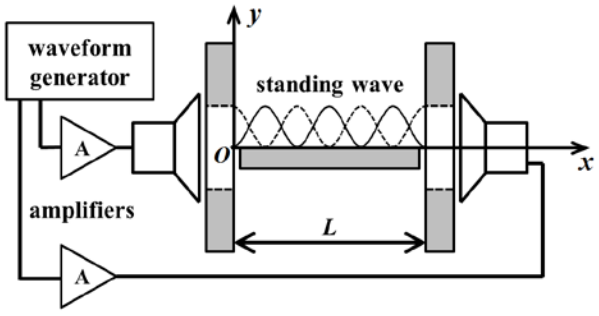

Fig. 3. A schematic diagram of an acoustic device for manipulating and sorting particles in air.

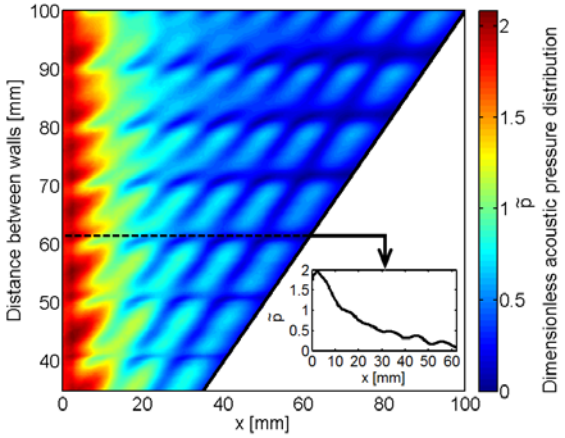

Fig. 4. Dimensionless acoustic pressure amplitude at a horizontal line located 2 mm above the glass plate as a function of x and L, in the case of only the left speaker being active. Inset figure presents the dimensionless pressure amplitude as a function of x for a distance between walls of 62 mm.

IV. RESULTS AND DISCUSSION

A. Dynamic acoustic field in liquids

To demonstrate how the DAF technique can be applied to sort particles by size, the finite-difference scheme was used to simulate the separation of polystyrene particles by size in water. The simulation parameters are presented in Table I.

TABLE I. Simulation parameters in liquid.

Parameters	values
ρ_w [kg/m^3] [27]	1000
β_w [Pa^{-1}] [27]	4.56 x 10^{-10}
ρ_c [kg/m^3] [28]	1050
β_c [Pa^{-1}] [28]	2.16 x 10^{-10}
η [Pa.s] [29]	1 x 10^{-3}
p_0 [kPa]	35
f [MHz]	4
t_{ramp} [s]	8
t_{rest} [s]	4

The simulated results of Fig. 5 illustrate the separation of polystyrene particles by size, showing the horizontal position of 10 and 45 μm diameter particles as a function of time. At t = 0, both particles are located at x = 0. Then the DAF technique is applied and the 45 μm particle starts following the moving node, whilst the 10 μm particle remains close to its initial position. After one full period (T = 12 s), the 45 μm particle originally located at x = 0 is displaced to x = 185 μm (λ/2), while the 10 μm particles moves only to a peak position of x = 26 μm during t_{ramp} and relaxes back to x = 0 during t_{rest}. By repeating the full period for a second time, the 45 μm particle moves from x = 185 μm to x = 370 μm (λ) and the 10 μm particle remains at x = 0. This clearly demonstrates how particles of varying size can be effectively separated. A supplementary video (supplementary video 2) shows the simulated acoustic separation of 10 and 45 μm polystyrene particles. In this supplementary video, the polystyrene particles are randomly positioned at t = 0. Then, a static acoustic field is applied for 10 s, forcing the particles to agglomerate at the pressure nodes. After a further 10 s, the

DAF starts, and separates the larger particles from the smaller ones.

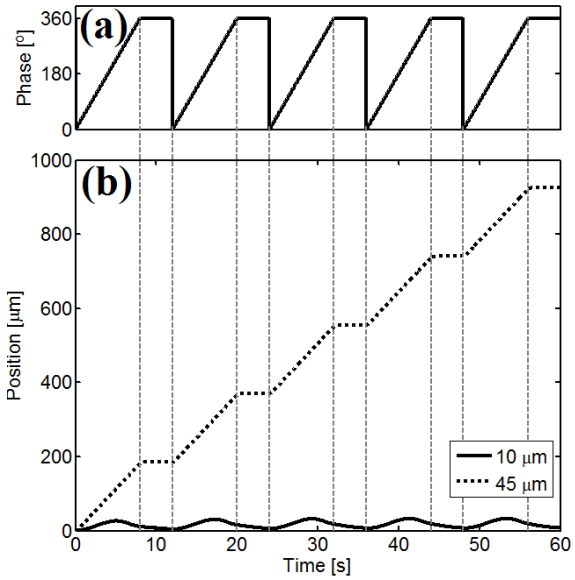

Fig. 5. Simulation of the dynamic acoustic field (DAF) technique for sorting polystyrene particles by size. In this simulation, particles of 10 and 45 µm diameter are separated. The simulation parameters used are presented in Table I.

To verify the discriminating capability of the DAF method experimentally, three sets of polystyrene particles varying in diameters (a) 10 and 45 µm, (b) 8 and 10 µm (supplementary video 3) and (c) 5 and 6 µm (Polysciences Europe, Germany) were submitted to the technique. The experiments were repeated 10 times for each sets. Polystyrenes particles were chosen as they are good surrogates for cells, and thus give a good approximation of cell behavior under acoustic field. The acoustic pressures were calculated for the polystyrene particles of 5, 6, 8, 10, and 45 µm in diameter and was found to be 4.8, 8.5, 9.4, 11.2, and 12.1 × 10^4 Pa, respectively.

To replicate biological experiments on sorting dorsal root ganglion cells from debris for regenerative medicine applications, the separation experiments were performed with each set of polystyrene particles containing a mixture ratio of 100:1 for the smaller / larger particles. In the heterogeneous cell mixture, the debris cells concentration is higher than dorsal ganglion cells [14]. The concentration of small particles was chosen just below aggregation of particles was observed. Particle movements were analyzed with Tracker software [30]. Figure 6 shows the particle displacement versus time under the DAF for each of the three different sets. As expected from the numerical model, the larger particles (trace in red) follow the DAF, whilst the smaller particles (trace in black) stay around their initial position.

Separation purity and separation efficiency are two figures of merit that can be used to assess separation performance. Achieving both high purity and efficiency of separation is not always possible. High separation efficiency is less important in most applications compared to high separation purity. The purity performance can be expressed as:

$$\text{Purity} = \frac{n_{\text{target}}}{n_{\text{total}}} \times 100\%, \quad (10)$$

where n_{target} is the number of target particles, n_{total} is the total particle number in the separated population.

The separation efficiency is expressed as:

$$\text{Efficiency} = \frac{n_{\text{captured}}}{n_{\text{introduced}}} \times 100\%, \quad (11)$$

where $n_{captured}$ is the number of particles retained in the separation medium and $n_{introduced}$ is the total particle number introduced in the system.

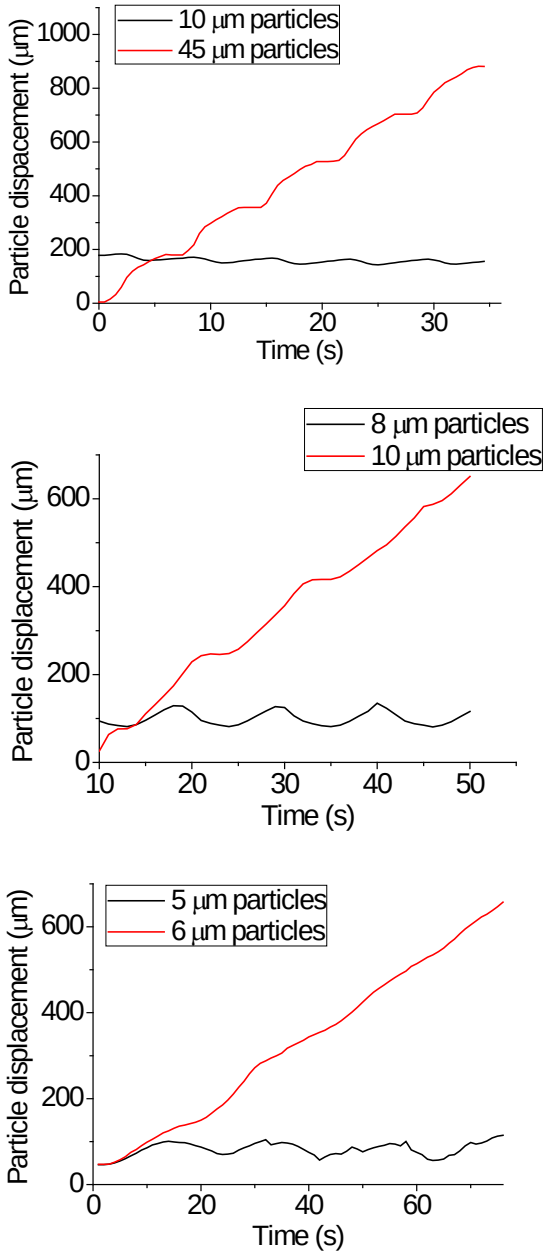

Fig. 6. The displacement vs. time for three different sets of polystyrene particles during the application of the dynamic acoustic field technique: (a) 10 and 45 µm in diameter, (b) 8 and 10 µm in diameter and (c) 5 and 6 µm in diameter.

To demonstrate the potential of the DAF technique, purity and efficiency were analyzed by measuring the movement of the three different sets of particles over five nodes. The effect of different t_{ramp} and t_{rest} were studied on each set of polystyrene particles, and purity and efficiency were analyzed, respectively. Details of the effect of t_{ramp} and t_{rest} on purity are discussed elsewhere [14]. The measurement results are reported in Table II and it focus mainly on high purity rather than efficiency. As it can be observed in Table II, purity and efficiency reach approximately 100% for a particle set of 10 and 45 µm. The results show that both efficiency and purity are reduced when decreasing the particle size difference. However, even for the set that only had 20 % difference in particle diameter (5 and 6 µm) results in ~ 85 % purity and ~ 50 % efficiency. Therefore, the DAF method has the potential for discriminating particles of different sizes even when this difference is relatively small.

TABLE II. Separation efficiency and separation purity for three different sets of polystyrene particles.

particles set	t_{ramp}/t_{rest}	Efficiency	Purity
10 µm / 45 µm	8 s / 4 s	~ 100 %	~ 100 %
8 µm / 10 µm	7.2 s / 3.8 s	~ 75 %	~ 85 %
5 µm / 6 µm	13.5 s / 5.7 s	~ 50 %	~ 85 %

B. Dynamic acoustic field in air

The acoustic device for manipulation in air was excited at a frequency of 17.5 kHz achieving a sound pressure of approximately 110 dB. According to the numerical simulation, there are six positions of minimum potential (see Fig. 7 (a)). When both speakers operate in phase, the positions of minimum Gor'kov potential were located at x = 3.9, 14.8, 25.8, 36.2, 47.2, and 58.0 mm. The distance between the positions of minimum Gor'kov potential varied between 10.4 and 11.0 mm, values that were slightly higher than half the wavelength ($\lambda/2$ = 9.7 mm). This slight difference occurs because the acoustic standing wave is not exactly a plane wave, as described by Xie and Wei [16].

The trapping of expanded polystyrene particles shown in Fig. 7 (b) was obtained by exciting the right and the left speakers in phase. By introducing, and varying, a phase difference between the speakers, particles could be manipulated along the x-axis. A shift in the phase difference causes the series of potential wells to be translated along the x-axis, allowing the particles to be manipulated. Assuming a quasi-static condition (i.e. the phase is altered slowly), we can consider that the particle position coincides with the node.

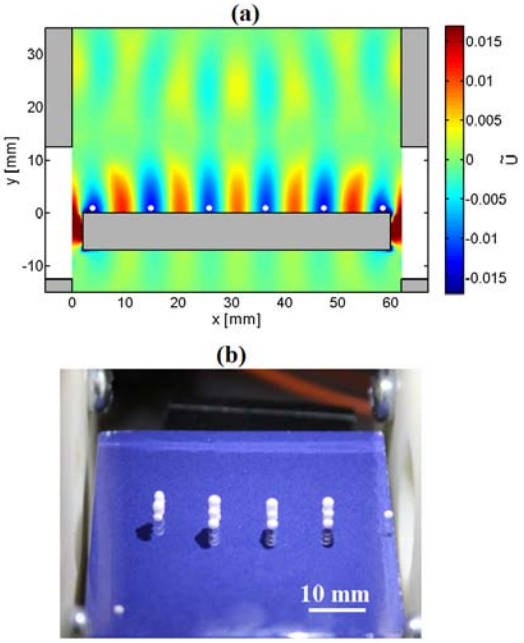

Fig. 7. (a) Simulated dimensionless Gor'kov potential. In this figure, the speakers (white bars at left & right) are excited in phase, particles are represented as white dots, and the glass plate is shown as a grey rectangle. (b) Optical image of the trapped expanded polystyrene particles in air at the pressure nodes of the acoustic standing wave formed by two speakers actuated in phase.

To demonstrate the sorting technique, expanded polystyrene particles with a density of 38 kg/m^3 and diameters of 2 and 5 mm were placed on the glass plate and the DAF cycling pattern (Fig. 1) was repeated three times, with t_{ramp} = 0.7 s and t_{rest} = 1.3 s. Figure 8 (supplementary video 4) shows the evolution of a pair of particles under the DAF. Initially, the 5 mm particle is located at the second potential well (x = 14.8 mm) and the 2 mm particle is located at the third one (x = 25.8 mm). After three cycles, the 5 mm particle is transported from the second to the fifth potential well (x = 47.2 mm), while the 2 mm particle remains trapped at the third potential well. We experimentally investigated several sets of parameters for t_{ramp} and t_{rest} and identified t_{ramp} = 0.7 s together with t_{rest} = 1.3 s as the optimum combination: particles of 5 mm diameter were transported whilst 2 mm diameter particles remained in place. The motion of the two particles was recorded by a digital camera and a video analysis software [27] was used to extract the particle positions as a function of time. If more particles are added to the experiments, the particles agglomerate with each other making the limitation in the sorting. Figure 8 also presents the positions of the minima of the Gor'kov potential obtained numerically. Table III describe the parameters used in the simulation in air. It can be seen, that the 5 mm particle followed the position of minimum Gor'kov potential, while the smaller particle was only slightly perturbed by the acoustic radiation force (supplemental material 4). During each DAF cycle of 2 s, the large particle is translated horizontally by a distance slightly larger than half wavelength. These experiments demonstrate the applicability of the DAF separation process in air. However, simulations

show that air drag force may not be sufficient to explain the separation process in air, which may result, in our case, from a complex combination of air drag force as well as friction and electrostatic force between particles and the glass surface, both of which are difficult to quantify. Friction and electrostatic forces involved in the separation of particles in air could be investigated by exploring different types of surfaces in order to control the adhesion forces between the particles and the surface. Although the acoustic separation in air was demonstrated with millimeter-sized particles, one can expect that the DAF technique can be used to sort micron-sized particles such as powders or aerosol, which has many potential applications in industry [31], [32].

TABLE III. Simulation parameters in air.

parameters	Values
ρ [kg/m^3] [17]	1.2
c [m/s] [17]	340
f [kHz]	17.5
t_{ramp} [s]	0.7
t_{rest} [s]	1.3

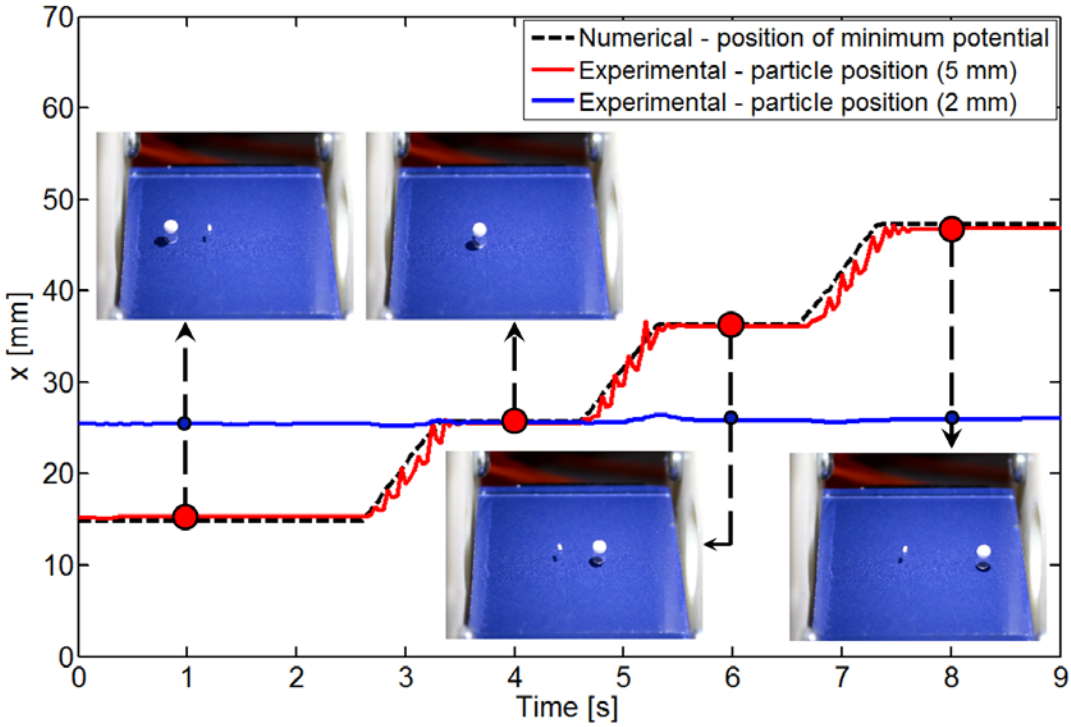

Fig. 8. Horizontal position of two expanded polystyrene particles (2 and 5 mm diameter) as a function of time. The graphic also presents the position of minimum Gor'kov potential as a function of time. A supplementary video demonstrating the dynamic sorting of particles is available online. The movement was non-uniform during translation due to the direct digital synthesis (DDS) technology used within the signal generator resulting in an uneven change of amplitude when the phase of the exciting signal is modulated. A video illustrating the separation of the particles is available as online supplemental video 4.

V. Conclusion

In this paper a dynamic acoustic field (DAF) technique was presented as a general method for manipulating and sorting particles. In a quasi-static condition, viscous drag forces can be neglected and particles can be manipulated horizontally by changing the phase difference between two emitters. By increasing the rate at which the phase is changed, viscous drag forces increase during particle movement, and produce a discriminating effect between small and large particles: larger particles follow the moving nodes, whereas smaller particles being only slightly perturbed by the dynamic acoustic field, remain close to their initial position. We demonstrate this approach by separating polystyrene particles by size in a liquid medium. The particle separation was performed up to a ratio of 5/6 in diameter (20 % diameter difference). Finally, to demonstrate that the capabilities and the scalability of the DAF technique are not restricted to liquid media, expanded polystyrene particles were manipulated and sorted in air.

References

[1] X. Ding, S. C. S. Lin, B. Kiraly, H. Yue, S. Li, I. K. Chiang, J. Shi, S. J. Benkovic, and T. J. Huang, "On-chip manipulation of single microparticles, cells, and organisms using surface acoustic waves," *Proc. Natl. Acad. Sci.*, vol. 109, no. 28, pp. 11105-11109, 2012.

[2] A. A. S. Bhagat, H. Bow, H. W. Hou, S. J. Tan, J. Han, C. T. Lim, "Microfluidics for cell separation," *Med. Biol. Eng. Comput.*, vol. 48, no. 10, pp. 999-1014, 2010.

[3] X. Ding, Z. Peng, S. C. S. Lin, M. Geri, S. Li, P. Li, Y. Chen, M. Dao, S. Suresh, and T. J. Huang, "Cell separation using tilted-angle standing surface acoustic waves," *Proc. Natl. Acad. Sci.*, vol. 111, no. 36, pp. 12992-12997, 2014.

[4] D. Foresti, M. Nabavi, M. Klingauf, A. Ferrari, and D. Poulikakos, "Acoustophoretic contactless transport and handling of matter in air," *Proc. Natl. Acad. Sci.*, vol. 110, no. 31, pp. 12549-12554, 2013.

[5] R. S. Budwig, M. J. Anderson, G. Putnam, and C. Manning, “Ultrasonic particle size fractionation in a moving air stream,” *Ultrasonics*, vol. 50, no. 1, pp. 26-31, 2010.

[6] K. E. McCloskey, J. J. Chalmers, and M. Zborowski, “Magnetic cell separation: characterization of magnetophoretic mobility,” *Anal. Chem.*, vol. 75, no. 24, pp. 6868-6874, 2003.

[7] R. Pethig, “Dielectrophoresis: status of the theory, technology, and applications,” *Biomicrofluidics*, vol. 4, no. 2, art. no. 022811, 2010.

[8] D. G. Grier, “A revolution in optical manipulation,” *Nature*, vol. 424, pp. 810-816, 2015.

[9] V. Marx, “Biophysics: using sound to move cells,” *Nat. Methods*, vol. 12, no. 1, pp. 41-44, 2015.

[10] A. L. Bernassau, F. Gesellchen, P. G. A. MacPherson, M. Riehle, and D. R. S. Cumming, “Direct patterning of mammalian cells in an ultrasonic heptagon stencil,” *Biomed. Microdevices*, vol. 14 no. 3, pp. 559-564, 2012.

[11] F. Gesellchen, A. L. Bernassau, T. Déjardin, D. R. S. Cumming, and M. O. Riehle, “Cell patterning with a heptagon acoustic tweezer”, Lab. Chip, vol. 14, no. 13, pp. 2266-2275, 2014.

[12] T. Laurell, F. Petersson, and A. Nilsson, “Chip integrated strategies for acoustic separation and manipulation of cells and particles,” *Chem. Soc. Rev.*, vol. 36, no. 3, pp. 492-506, 2007.

[13] F. Petersson, A. Nilsson, C. Holm, H. Jönsson, and T. Laurell, “Separation of lipids from blood utilizing ultrasonic standing wave fields in microfluidic channels,” *Analyst*, vol. 129, pp. 938-943, 2004.

[14] G. D. Skotis, D. R. S. Cumming, J. N. Roberts, M. O. Riehle, and A. L. Bernassau, “Dynamic acoustic field activated cell separation (DAFACS)”, Lab. Chip, vol. 15, pp. 802-810, 2015.

[15] G. Whitworth and W. T. Coakley, “Particle column formation in a stationary ultrasonic field,” *J. Acoust. Soc. Am.*, vol. 91, no. 1, pp. 79-85, 1992.

[16] W. J. Xie and B. Wei, “Parametric study of single-axis acoustic levitation,” *Appl. Phys. Lett.*, vol. 79, no. 6, pp. 881-883, 2001.

[17] M. A. B. Andrade, F. Buiochi, and J. C. Adamowski, “Finite element analysis and optimization of a single-axis acoustic levitator,” *IEEE Trans. Ultrason. Ferroelectr. Freq. Control*, vol. 57, no. 2, pp. 469-479, 2010.

[18] T. Kozuka, T. Tuziuti, H. Mitome, and T. Fukuda, “Non-contact micromanipulation using an ultrasonic standing wave field,” in The Ninth Annu. Int. Workshop on Micro Electro Mechanical Systems, 1996, pp. 435-440.

[19] P. Glynne-Jones, R. J. Boltryk, N. R. Harris, A. W. J. Cranny, M. Hill, “Mode-switching: A new technique for electronically varying the agglomeration position in an acoustic particle manipulator,” *Ultrasonics*, vol. 50, no. 1, pp. 68-75, 2010.

[20] A. Grinenko, C. K. Ong, C. R. P. Courtney, P. D. Wilcox, and B. W. Drinkwater, “Efficient counter-propagating wave acoustic micro-particle manipulation,” *Appl. Phys. Lett.*, vol. 101, no. 23, art. no. 233501, 2012.

[21] T. Kozuka, K. Yasui, T. Tuziuti, A. Towata, and Y. Iida, “Noncontact acoustic manipulation in air,” *Jpn. J. Appl. Phys.*, vol. 46, no. 7B, pp. 4948-4950, 2007.

[22] A. L. Bernassau, C. R. P. Courtney, J. Beeley, B. W. Drinkwater, and D. R. S. Cumming, “Interactive manipulation of microparticles in an octagonal sonotweezer,” *Appl. Phys. Lett.*, vol. 102, no. 16, art. no. 164101, 2013.

[23] C. R. P. Courtney, C. K. Ong, B. W. Drinkwater, A. L. Bernassau, P. D. Wilcox, and D. R. S. Cumming, “Manipulation of particles in two dimensions using phase controllable ultrasonic standing waves,” *Proc. R. Soc. A.*, vol. 468, no. 2138, pp. 337-360, 2012.

[24] H. Bruus, “Acoustofluidics 7: The acoustic radiation force on small particles,” *Lab Chip*, vol. 12 no. 6, pp. 1014-1021, 2012.

[25] L. P. Gor’kov, “On the forces acting on a small particle in an acoustic field in an ideal fluid,” *Sov. Phys. Dokl.*, vol. 6, no. 9, pp. 773-775, 1962.

[26] A. L. Bernassau, P. Glynne-Jones, F. Gesellchen, M. Riehle, M. Hill, and D. R. S. Cumming, “Controlling acoustic streaming in an ultrasonic heptagonal tweezers with applications to cell manipulation,” *Ultrasonics*, vol. 54, no. 1, pp. 268-274, 2014.

[27] S. W. Wenzel and R. M. White, “A multisensor employing an ultrasonic lamb-wave oscillator”, IEEE Trans. Electron Devices, vol. 35, no. 6, pp. 735-743, 1988.

[28] D. Hartono, Y. Liu, P. L. Tan, X. Y. S. Then, L. Y. L. Yung, and K. M. Lim, “On-chip measurements of cell compressibility via acoustic radiation”, Lab. Chip, vol. 11, no. 23, pp. 4072-4080, 2011.

[29] K. Yasuda, S Umemura, and K. Takeda, “Particle separation using acoustic radiation force and electrostatic force,” *J. Acoust. Soc. Am.*, vol. 99, no. 4, pp. 1965-1970, 1996.

[30] D. Brown, Tracker video analysis and modelling tool. Available at “https://www.cabrillo.edu/~dbrown/tracker/”

[31] W. Peukert and C. Wadenpohl, “Industrial separation of fine particles with difficult dust properties,” *Powder Technol.*, vol. 118, no. 1, pp. 136-148, 2001.

[32] A. Bürkholz, “Measurement and separation of very fine liquid and solid particles in the chemistry industry,” *J. Aerosol Sci.*, vol. 22, pp. S513-S516, 1991.